International Journal of Pharmaceutics 618 (2022) 121623

Contents lists available at ScienceDirect

International Journal of Pharmaceutics

journal homepage: www.elsevier.com/locate/ijpharm

Impact of anti-PDGFRα antibody surface functionalization on LNC uptake by oligodendrocyte progenitor cells

Yasmine Labrak [a,b], Béatrice Heurtault [c], Benoît Frisch [c], Patrick Saulnier [d], Elise Lepeltier [d], Veronique E Miron [e,f], Giulio G. Muccioli [b,*], Anne des Rieux [a,*]

[a] Université catholique de Louvain (UCLouvain), Louvain Drug Research Institute, Advanced Drug Delivery and Biomaterials, 1200 Brussels, Belgium
[b] Université catholique de Louvain (UCLouvain), Louvain Drug Research Institute, Bioanalysis and Pharmacology of Bioactive Lipids, 1200 Brussels, Belgium
[c] Université de Strasbourg, CNRS, Laboratoire de Conception et Application de Molécules Bioactives UMR 7199, Faculté de Pharmacie, 74 route du Rhin, 67401 Illkirch Cedex, France
[d] Université d'Angers, Unité de Micro et Nanomédecines Translationnelles, Inserm 1066, CNRS 6021, Institut de Biologie en Santé PBH-IRIS, 49033 Angers, France
[e] UK Dementia Research Institute at The University of Edinburgh, Centre for Discovery Brain Sciences, University of Edinburgh, Edinburgh, UK
[f] Medical Research Council Centre for Reproductive Health, University of Edinburgh, Edinburgh UK

ARTICLE INFO

Keywords:
Surface modification
Multiple sclerosis
Nanomedicines
Remyelination
Central nervous system
lipid nanoparticles

ABSTRACT

Impairment of oligodendrocyte progenitor cell (OPC) differentiation into oligodendrocytes and chronic inflammation are key determinants of poor remyelination observed in diseases such as multiple sclerosis. For many pro-myelinating molecules, the therapeutic potential is hindered by poor solubility or limited access to the targeted cells. A promising approach to improve the delivery of those molecules to OPC is to encapsulate them in functionalized Lipid Nanocapsules (LNC). We aimed to develop the first OPC-targeting LNC, by grafting an anti-PDGFRα antibody on the surface of the LNC using several strategies and evaluating the interaction with PDGFRα via ELISA. We found that only site-selective click-chemistry grafting maintained anti-PDGFRα/PDGFRα association, which was confirmed *in vitro* on primary rat OPC. In conclusion, we demonstrated that it was possible to produce anti-PDGFRα functionalized LNC, we confirmed the antibody's ability to recognize its receptor after grafting and we optimized techniques to characterize antibody functionalized LNC.

1. Introduction

The myelin sheath, formed by oligodendrocytes in the central nervous system (CNS), is a crucial element in the transduction of electrical impulses along the axons and in neuron metabolic support. In demyelinating diseases, such as multiple sclerosis (MS), loss of the myelin sheath causes invalidating symptoms such as cognitive dysfunction, impaired locomotor function and disorders such as optical neuritis (Dobson and Giovannoni 2019). In MS, demyelination results from a complex physiopathological process involving a targeted immune response towards the myelin sheath (Franklin and Ffrench-Constant 2017). Until now, the trigger of this autoimmune disease is still unknown, but the onset of MS is believed to be multifactorial (i.e. genetic, environmental, hypovitaminosis D, viral infections) (Filippi et al. 2018).

Endogenous repair of myelin sheaths occurs via the recruitment and differentiation of oligodendrocyte progenitor cells (OPC) into new myelinating oligodendrocytes (Franklin and Ffrench-Constant 2017). As a result, a new functional myelin sheath is rebuilt around axons, restoring efficient electrical impulse conduction. However, with time and MS progression, this mechanism becomes less efficient, mostly due to a limited oligodendrocyte repopulation and a thinner de novo myelin sheath (Franklin and Ffrench-Constant 2017; Dendrou, Fugger, and Friese 2015).

Most MS therapies focus on reducing peripheral inflammation and on lengthening remission time between relapses. However, no treatments stimulating remyelination are currently available (Göttle et al. 2019). To reach this goal, one strategy is to enhance remyelination by promoting OPC differentiation into mature oligodendrocytes (Lubetzki et al. 2020).

Abbreviations: Ab, anti-PDGFRα antibody; DBCO, Dibenzocyclooctyne; FACS, fluorescence associated cell sorting; IMT, 2-Iminothiolane•HCl; LNC, lipid nanocapsule; MFI, mean fluorescence intensity per cell; MS, multiple sclerosis; PDGFRα, platelet-derived growth factor receptor α; PDGFAA, platelet-derived growth factor A; OPC, oligodendrocytes progenitor cells.

* Corresponding authors.
E-mail addresses: giulio.muccioli@uclouvain.be (G.G. Muccioli), anne.desrieux@uclouvain.be (A. des Rieux).

https://doi.org/10.1016/j.ijpharm.2022.121623
Received 27 October 2021; Received in revised form 22 February 2022; Accepted 23 February 2022
Available online 26 February 2022
0378-5173/© 2022 Elsevier B.V. All rights reserved.

For the last decades, researchers have been working to decipher OPC differentiation pathways to find molecules that would enhance remyelination (Lubetzki et al. 2020). A few drugs have been tested in preclinical or clinical settings in this context. For instance, retinoic acid and calcitriol have been studied *in vitro* for their differentiating potential of OPC. Bexarotene, a lipophilic retinoid X receptor gamma (RXRγ) agonist, showed some interesting results on remyelination in a recent clinical trial involving relapsing-remitting MS patients (Brown et al. 2021). However, the trial was interrupted due to two major off-target effects, hypothyroidism and hypertriglyceridemia.

Using targeted nanomedicines is one strategy to reduce side effects. In this context, lipid nanocapsules (LNC) are gaining interest. Indeed, LNC are very efficient in solubilizing lipophilic bioactive drugs, are biocompatible, can protect their cargo from degradation and facilitate their transport across membranes (Roger et al. 2017). Moreover, their surface can be modified to favor their interactions with a specific cell or tissue. For instance, LNC surface has been modified to target a specific cell type (Carradori et al., 2016a); Hirsjarvi et al. 2014; Laine et al. 2012; Morille et al. 2009), mainly by adsorption of a targeting peptide ((Carradori et al., 2016a); Gazaille et al. 2021; Umerska et al. 2016). As platelet-derived growth factor receptor α (PDGFRα) is specifically expressed at the at the surface of OPCs in the CNS (Li et al. 2017; Zou et al. 2008), we hypothesized that grafting an anti-PDGFRα antibody at LNC surface would favor the targeting of OPC.

Thus, here we compared three different approaches to graft an anti-PDGFRα at LNC surface (LNC-Ab). Two are based on thiol-maleimide chemistry but involved different approaches to link the maleimide at LNC surface (transacylation vs post-insertion), while the third one is based on copper less click-chemistry. Following an extensive characterization of the obtained LNC-Ab, we assessed their targeting ability, first using a custom-made ELISA assay and then *in vitro*, in rat OPC primary cultures.

2. Materials and methods

2.1. Materials

Labrafac® provided by Gattefosse SA (France) and Lipoïd® S100 by Lipoid Gmbh (Germany). Kolliphor HS15®, poly-D-Lysine hydrobromide (70000–150000 Da), fluorescamine, 2-Iminothiolane•HCl and propidium iodide were purchased from Sigma (United-States). 1,2-Distearoyl-*sn*-glycero-3-phosphorylethanolamine-PEG $_{(2000)}$-Maleimide (DSPE-PEG-Maleimide) and NH_2-PEG$_{(5000)}$- Dibenzocyclooctyne (NH_2-PEG-DBCO) were purchased from Nanocs (United-States). NH_2-PEG $_{(5000)}$-Maleimide was purchased from Creative PEGWorks (United-States). Anti-PDGFRα was purchased from BioLegend (United-States). Anti-rat-HRP, DMEM (41966–029), HEPES, Pen/Strept, DMEM 0.05% trypsin-EDTA (1x), Presto blue Cell Viability Reagent, DiD'solid, SiteClick™ Antibody Azido Modification Kit and Alexa-488-Phalloidine were purchased from Thermo Fisher Scientific (United-States). Platelet-derived growth factor A (PDGFAA) and fibroblast growth factor 2 (FGF) were purchased from Peprotech (United Kingdom). rmPDGFRA/Fc chimera (soluble PDGFRα) has been purchased from R&Dsystems. Spectra-Por Float-a-lyzer G2 300 kDa dialysis membrane and Rotilabo® syringe sterile 0.22 µm filters were purchased from Carl Roth GmbH (Germany).

2.2. Preparation of anti-PDGFRα-lipid nanocapsules (LNC-Ab)

2.2.1. Preparation of the LNC

LNC were prepared following the protocol developed by Heurtault et al. (Heurtault et al. 2002). Briefly, 0.846 g of Solutol HS15, 0.075 g of Lipoïd®, 0.089 g of NaCl, 1.028 g of Labrafac® and 2.962 ml of water were mixed under magnetic stirring for 5 min at 50 °C. Next, three temperature cycles of heating/cooling were done between 60 °C and 90 °C, also under magnetic stirring. During the cooling of the last cycle, at 77 °C, 12.5 ml of cold water (4 °C) were added, under high-speed stirring. The resulting nanoparticle of 126 mg/ml were filtered with a 0.2 µm filter for sterilization and stored at 4 °C until use. LNC concentration was calculated by the total weight of Kolliphor HS 15, Lipoïd® and Labrafac® divided by the final volume the LNC formulation (Xu et al. 2018).

Fluorescent LNC, obtained by loading DiD into LNC (14,7 µg/ml of DID in LNC), were used for confocal and uptake experiments (Bastiat et al. 2013). DiD was added before the heating/cooling cycles.

2.2.2. Preparation of LNC-PEG-Maleimide

To graft Ab on the surface of the LNC, two approaches based on the coupling between thiol and maleimide moieties were used. The first one consisted of the transacylation of PEG chains (Kolliphor) exposed at LNC surface using NH_2-PEG-Maleimide (Approach 1), while the second one consisted of the post-insertion of DSPE-PEG-Maleimide in the PEG corona of the LNC (Approach 2) (Fig. 1A). For both approaches, the thiolated antibody was covalently coupled to the PEG by reaction with the maleimide moiety.

Transacylation of NH_2-PEG-Maleimide (Approach 1): Transcylated LNC were made according to Messaoudi et al.'s protocol (Messaoudi et al. 2014). Briefly, 5 mg of NH_2-PEG-Maleimide (1:100, molar ratio of Maleimide : Kolliphor HS®) with 2 ml of LNC and 100 µl of NaOH (10 M) were incubated under agitation for 15 min. Then 2 ml of glycine buffer (50 mM of glycine and 5 mM of HCl, pH = 2) were added. NH_2 reacted with the hydroxystearic acid moiety of the Kolliphor HS®, to form an amide bond linking the LNC to the NH_2-PEG-Maleimide. After NH_2-PEG-Maleimide covalent grafting at the surface of the LNC, the formulation was dialyzed for 48 h (cut-off 300 kDa) against water to remove the unbound PEG-maleimide.

Post-insertion of DSPE-PEG-Maleimide (Approach 2): Post-inserted LNC were made according to Perrier et al. protocol (Perrier et al. 2010). Briefly, DSPE-PEG-Maleimide (1:100 M Ratio of PEG-Maleimide: Kolliphor HS®) dissolved in PBS was incubated for 1 h at 60 °C under agitation. Afterward, 300 µl of this solution were added to 400 µl of LNC prepared as described in section 2.2.1. The resulting mixture underwent seven cycles of 15 min incubation at 60 °C under stirring followed by 15 min of incubation on ice.

2.2.3. Preparation of LNC-PEG-DBCO

NH_2-PEG-DBCO was covalently grafted to the surface of the LNC by transacylation as described in section 2.2.2 (Approach 3) (Fig. 2). Five mg or 10 mg of NH_2-PEG-DBCO (1:100 or 1:50 M ratio of PEG-DBCO : Kolliphor HS®) with 2 ml of LNC and 100 µl of NaOH (10 M) were incubated under agitation for 15 min. Then, LNC-PEG-DBCO were separated from unreacted components as described in 2.2.2.

2.2.4. Grafting of anti-PDGFRα on LNC

2.2.4.1. For LNC-PEG-Maleimide (Approach 1 and 2). The primary amines on the anti-PDGFRα (Ab) were thiolated with 2-iminothiolane•HCl (IMT) in PBS (Fig. 1). A mixture of Ab and IMT was made using a molar ratio Ab:IMT of 10:1, with a concentration of IMT of 13.7 µg/ml. Ab and IMT were kept under agitation for 1 h during which the solution was vortexed every 15 min (Behzadi et al. 2017). Then, 200 µl of LNC were mixed with 100 µl of the Ab : IMT solution and incubated under agitation for 2 h (vortexed every 30 min). To block the remaining free maleimide at the LNC surface, cysteine•HCl was added to the suspension and was further incubated for 30 min. The resulting suspension was dialyzed for 48 h (cut-off 300 kDa) to remove unbound Ab.

2.2.4.2. For LNC-PEG-DBCO (Approach 3). According to supplier instructions, Ab and anti-IgG2a were azido-modified using the Thermofisher® Site-Click kit (Fig. 2). Briefly, a β-galactosidase enzyme was used to remove the terminal galactose residues of the carbohydrate chains localized on the Fc region of the antibody. Those terminal residues were

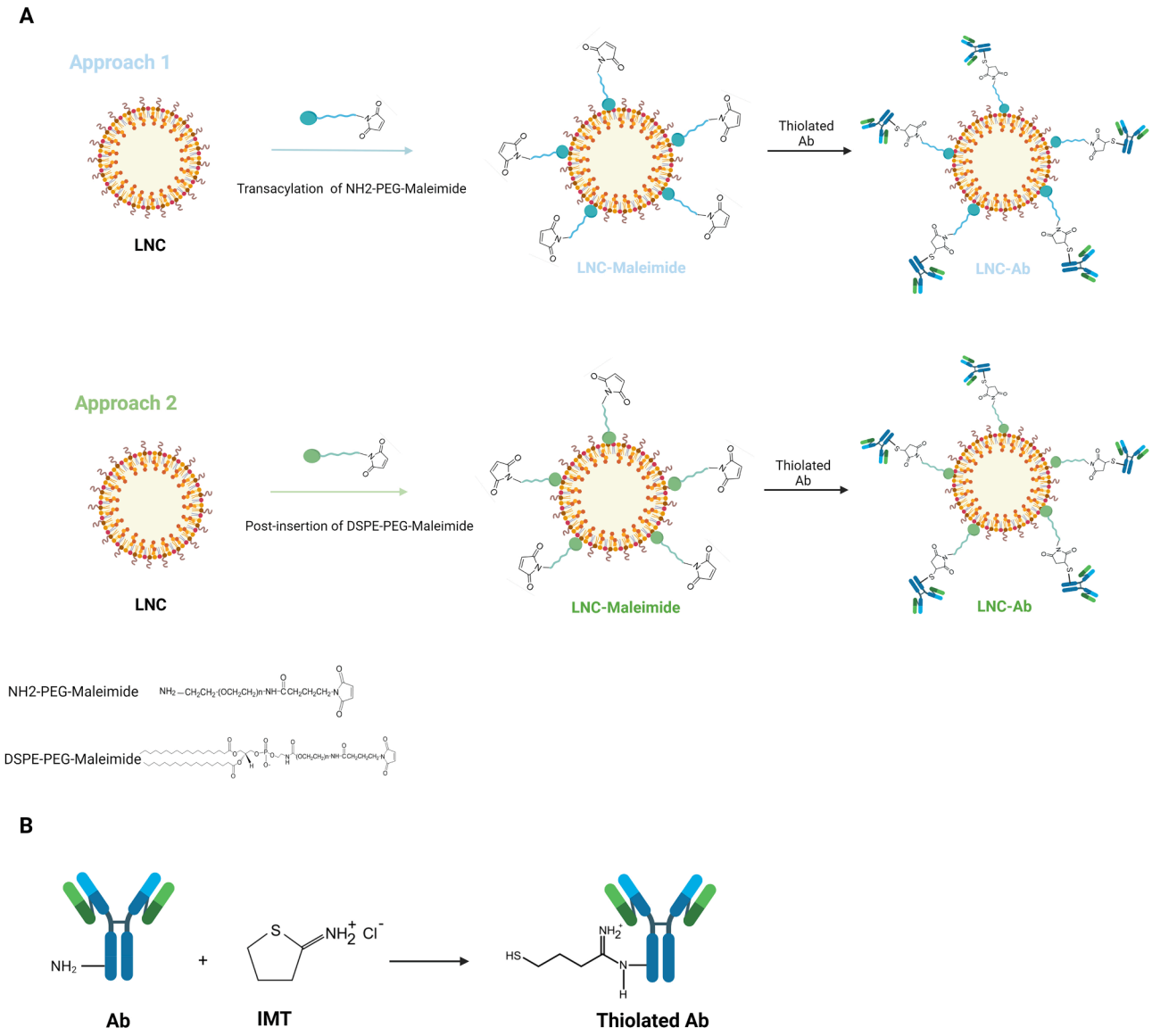


Fig. 1. Preparation of LNC-PEG-Maleimide and grafting of Ab (A) The PEG-Maleimide conjugate was added at the surface of the LNC using two different approaches: Approach 1 consisted of the transacylation of NH_2-PEG-Maleimide, and Approach 2 involved the post-insertion of DSPE-PEG-Maleimide. Both led to the formation of LNC-Maleimide. (B) The Ab (anti-PDGFRα) was thiolated by using IMT (2-iminothiolane•HCl). Then, the thiolated Ab formed a thioether bond with the maleimide moiety present at LNC surface. Unattached Ab were removed by dialysis. (created with Biorender.com)

replaced by an azide-containing sugar (GalNAz) using a β-1,4-galactosyltransferase. Then 200 µl of LNC were incubated overnight with 100 µl of a solution containing 280 µg/ml of azido modified antibody diluted in PBS. According to the manufacturer, the average number of DBCO moieties per antibody was 3 to3.5. The resulting suspension was dialyzed for 48 h (cut-off 300 kDa) to remove unbound Ab.

2.3. Characterization of LNC-Ab

Size, polydispersity index and zeta potential of LNC-Ab were measured in milliQ water using a ZetasizerUltra® (Malvern, United Kingdom).

To determine the antibody grafting yield, following removal by dialysis of the unbound Ab from the LNC preparation (see above), primary amines of the Ab were quantified with a fluorescamine assay (Schelte et al. 2000; Udenfriend et al. 1972). Briefly, 50 µl of LNC-Ab were mixed with 50 µl of HCl 12 M and incubated for 12 h at 120 °C to hydrolyze the peptidic bonds. After heating, 100 µl of NaOH 6 M were added to the mixture. Five hundred µl of a fluorescamine solution (30 mg/100 ml of dioxane), 1,5 ml of borate buffer (pH = 9, 45 mM of boric acid and 76 mM of borate) and 40 µl of sample were mixed in a quartz cuvette extemporaneously and resulting fluorescence was read at λex = 400 nm and λem = 480 nm (Spectramax® reader, Molecular Device®, United Kingdom). The calibration curve was produced using increasing amounts of Ab (2.25 to 27.5 µg/ml) in the presence of LNC as a matrix. A representative calibration curve can be found in the supplementary data (Fig. 1.S). The detection limit and the quantification limit of the method are 2.83 µg/ml and 9.83 µg/ml, respectively. The intraday day precision was 8.2% and 5.4%, and the interday precision was 6.8% and 4.5 %, when using 13.7 µg/ml and 27,5 µg/ml, respectively. The calculated accuracy is of 8.7%, and 3.5 % for 13.7 µg/ml and 27,5 µg/ml, respectively.

To determine the amount of antibody, present in the LNC-Ab, the samples were prepared similarly to the calibration curve, where an increasing quantity of sample was reacted with fluorescamine, resulting in a sample curve that follows the equation

$Y = ax$. Grafting efficiency was then calculated with the following equation:

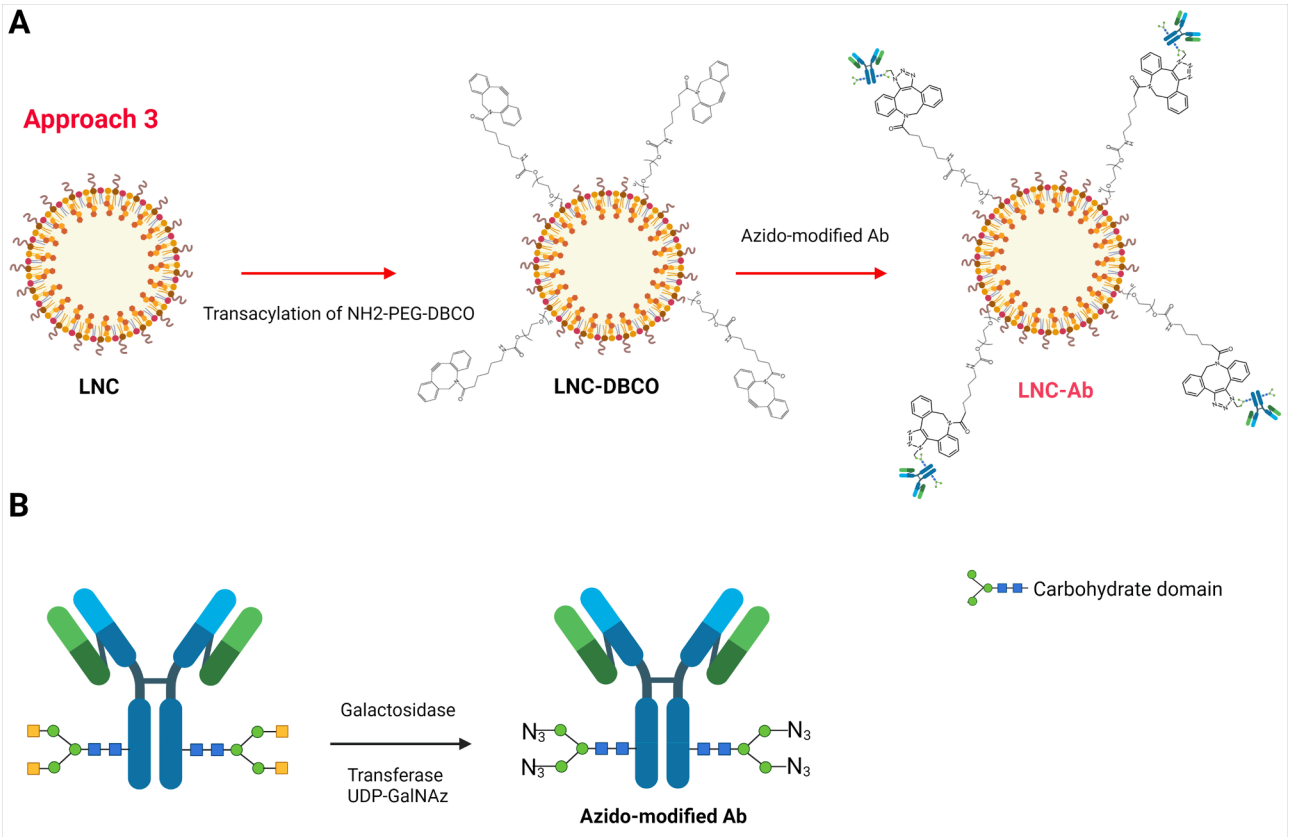


Fig. 2. Preparation of LNC-PEG-DBCO and grafting of Ab (A) A transacylation reaction was used to add the NH_2-PEG-DBCO conjugate at LNC surface. (B) The azide moiety was added on Ab using the Thermofisher® Site-Click kit. The modification was made on the carbohydrate chains of the Fc region of the Ab specifically. The DBCO alkyne reacted with the Ab azide to form a triazole bond, linking the Ab covalently to the LNC. (created with Biorender.com)

$$Grafting\ efficiency(\%) = \frac{Slope\ of\ Sample\ curve}{Slope\ of\ Calibration\ curve} * 100$$

To obtain an estimation of the number of antibodies per LNC, the quantity of antibody was divided by the number of LNC in the sample (Table 1.S; measured by nanoparticle tracking analysis (NTA) (Zetaview®, Particle Metrix®, Germany)) using the following equations:

$$Quantity\ of\ Ab\ (g) = Amount\ of\ Ab\ introduced\ in\ LNC(g) \times Grafting\ efficiency$$

$$Total\ number\ of\ Ab\ in\ the\ formulation = \frac{quantity\ of\ Ab \times Na}{Molecular\ weight\ of\ Ab}$$

$$Number\ of\ Ab\ per\ LNC = \frac{Amount\ of\ Ab\ per\ L}{Number\ of\ particles\ per\ L}$$

Na: Avogadro number $= 6.022 \times 10^{23}\ mol^{-1}$
Molecular weight of Ab $= 150000\ g.mol^{-1}$

2.4. Impact of the grafting on the interaction of anti-PDGFRα with its target

The impact of the grafting on Ab ability to interact with its target has been assessed by an ELISA optimized in our lab. A 96-well plate was coated with 100 µl of soluble PDGFRα (rmPDGFRα) diluted at different concentrations (from 0.3 to 20 nM) in PBS and incubated overnight at 4 °C. Then, the plate was washed 3 times and blocked with 300 µl of a 1% BSA solution in PBS during 1 h. Then, LNC-Ab and all other conditions were diluted in a 0,1% BSA solution at 1 nM of Ab. Following 4 h of incubation at room temperature and 3 washes, 100 µl of anti-rat-HRP antibody (1:2000 dilution) were added to the wells and incubated for 1 h at RT. TMB (3,3′,5, 5′- tetramethylbenzidine) was used as HRP substrate, and the optical density was read at 450 nm.

The Ab /rmPDGFRα association was appreciated by calculating the percentage of Ab response rate using the following equation:

$$\%response\ rate = \frac{OD_{450}\ of\ modified\ Ab\ at\ 20nM}{OD_{450}\ of\ unmodified\ Ab\ at\ 20nM} * 100$$

where a response rate of 100% would correspond to a similar recognition of the rmPDGFRα by the modified Ab and the commercial Ab.

To evaluate PEG chain impact on Ab activity, the Ab was pegylated according to the protocols used for Approach 1 and 3.

2.4.1. Pegylation of Ab with NH_2-PEG-Maleimide

The primary amines on the anti-PDGFRα (Ab) were thiolated with 2-Iminothiolane•HCl (IMT) in PBS (Fig. 1). A mixture of Ab and IMT was made using a molar ratio Ab:IMT of 10:1, with a concentration of IMT of 13.7 µg/ml. Ab and IMT were incubated under agitation for 1 h during which the solution was vortexed every 15 min (Behzadi et al. 2017). Then, 200 µl of a NH_2-PEG-Maleimide solution (1.25 mg/ml in MilliQ water) were mixed with 100 µl of the Ab: IMT solution and incubated under agitation for 2 h (vortexed every 30 min).

2.4.2. Pegylation of Ab with NH_2-PEG-DBCO

According to supplier instructions, Ab and anti-IgG2a were azido-modified using the Thermofisher® Site-Click kit (Fig. 2). Briefly, a β-galactosidase enzyme was used to remove the terminal galactose residues of the carbohydrate chains localized on the Fc region of the antibody. Those terminal residues were replaced by an azide-containing sugar (GalNAz) using a β-1,4-galactosyltransferase. Then 200 µl of a NH_2-PEG-DBCO solution (1,25 mg/ml in MilliQ water) was incubated

with 100 µl of a solution containing 280 µg/ml of azido modified antibody diluted in PBS.

2.5. OPC primary culture

Cortical mixed glial cultures were generated from Sprague-Dawley rat pups (postnatal day 0–2), according to Directive 2010/63/EU, to guidelines of the Belgian Government following the approval by the ethical committee for animal care of the faculty of medicine of UCLouvain (2017/UCL/MD/030), as described previously by Miron et al (Miron et al. 2013). Briefly, brains were dissected and the cerebellum, olfactory bulbs, and meninges were removed. Brains were then digested using papain (40 µg/ml) and platted in T75 flasks, for 10 days, in DMEM containing 4.5 g l^{-1} glucose, L-glutamine, pyruvate, 10% fetal calf serum (vol/vol) and 1% penicillin/streptomycin (vol/vol). To remove microglia, flasks were shaken on a rotary shaker at 230 rpm (1 h, 37 °C). After addition of 10 ml of fresh media, OPC were retrieved after further agitation (16 h on a rotary shaker at 37 °C at 220 rpm). OPC were then pelleted (250xg for 5 min) and plated at 1×10^4 cells/well in poly-D-Lysine coated (4µg/ml) 96 well plates Tc treated (BD Falcon) or 12 well plates. The medium consisted in DMEM containing 4.5 g/L glucose, L-glutamine, pyruvate, SATO (16 µg/ml putrescine, 400 ng/ml L-thyroxine, 400 ng/ml tri-iodothyroxine, 60 ng/ml progesterone, 5 ng/ml sodium selenite, 100 µg/ml bovine serum albumin fraction V, 10 µg/ml insulin, 5.5 µg/ml halo-transferrin (all from Sigma-Aldrich)), 0.5% fetal calf serum 1% penicillin/streptomycin, 10 ng/ml PDGFAA, and 10 ng/ml FGF. For experiments with depleted PDGFAA media, PDGFAA was removed 18 h prior to LNC treatment.

2.6. LNC cytotoxicity on OPC

LNC were diluted at different concentrations (0.63 mg/ml to 0.15 mg/ml) in OPC medium and were incubated for 1 h, 4 h and 24 h with OPC 2 days post-seeding. The media was then removed and replaced with fresh OPC medium containing 10% of PrestoBlue® Cell Viability Reagent. After 18 h of incubation, the fluorescence was read at λex = 530 nm and λem = 580 nm. Untreated OPC were used as positive control (100 % viability).

2.7. LNC-Ab association with OPC

2.7.1. Confocal microscopy

Cells were seeded in 96 well plates and were treated 2 days after seeding with LNC (DiD)-Ab for 30 min, at the concentration of 0.42 mg/ml. Then, they were washed once before fixation (15 min, PFA 4%). After fixation, cells were washed 3 times with PBS, blocked and permeabilized using PBS containing 5% normal goat serum and 100 µg/ml digitonin. Cells were then washed gently 3 times with PBS and were incubated 30 min with Phalloidine-488 (1:100) diluted in PBS 1% Normal goat serum for 30 min. Cells were then washed 3 times and kept in PBS. Images were taken using a Cell Observer Spinning Disk Confocal microscope (ZEISS) and a 40x oil objective.

2.7.2. Fluorescence associated cell sorting (FACS)

Cells were seeded and treated in 12-well plates, with either LNC (DiD)-Ab or LNC (DiD)-IgG2a isotype or LNC (DiD). The nanoparticles were diluted at a concentration of 0.15 mg/ml in complete DMEM media and incubated with OPC for 30 min. After incubation, the media was removed, and cells were rinsed with Dulbecco's phosphate-buffered saline. To detach the cells, 500 µl of DMEM 0,05% trypsin-EDTA were added into each well and incubated at 37 °C for 8 min. Cells were then pelleted (300xg for 5 min) and washed in FACS buffer (0.1% BSA and 1 mM EDTA in PBS). Dead cells were excluded from the analysis based on Propidium iodide staining. To differentiate DiD^+ cells from DiD^- ones, cells that were not incubated with LNC were used as control. Samples were analyzed with a BD FACSverse™. Flow cytometry data were treated with the Flowjo® software.

2.8. Statistical analysis

T-tests, one-way ANOVA and two-way ANOVA were performed using PRISM version 9 (GraphPad Software, United-States) to determine statistical significance. Results were considered significant if $p < 0.05$. N indicates the number of independent experiments and n the number of replicates. Detailed information about the number of replicates and the statistical test applied can be found in figure captions.

3. Results

3.1. Characterization of LNC-Ab obtained with the maleimide coupling strategy

LNCs had a size of 58 nm, a PDI of 0.04 and a zeta potential of −3 mV (Fig. 3). The addition of maleimide moieties on LNCs surface with approach 1 significantly increased their size (+9 nm) and decreased their zeta potential (from −3 to −24 mV). The second approach increased LNC size (+13 nm), although it did not significantly impact the zeta potential (-3 to −8 mV). The PDI was < 0.2 for all these formulations. Grafting the Ab on LNC-Maleimide had no impact on their size and PDI, while it impacted LNC zeta potential for approach 2 (-8 mV vs −24 mV).

3.2. Impact of PEG-Maleimide insertion method on Ab grafting efficiency

The average number of Ab grafted at LNC surface was quantified using a primary amine quantification assay developed by Schelté et al. (Schelte et al. 2000). Approach 1 resulted in a higher number of antibodies at the nanoparticle's surface, with an estimate of 49 Ab per LNC, than approach 2 where an average of 7 Ab per LNC was detected (Table 1). Since approach 1 provided the highest grafting efficiency, it was selected for the next step.

3.3. Impact of grafting on the interaction between anti-PDGFRα and PDGFRα

As grafting could modify Ab interaction with its receptor, the objective of this part was to evaluate if LNC-Ab had the same degree of interaction with its receptor than the unmodified Ab. We also evaluated if LNC would interfere with the ELISA signal by using the same concentration of Ab diluted in LNC (Ab + LNC) but there was no significant change on the biding curve, meaning that LNC did not interfere with the assay (Fig. 4).

While mixing LNC with Ab and Ab thiolation (Ab-SH) did not impact their interaction with the rmPDGFRα, covalently grafting the Ab on LNC surface (with approach 1) impaired its ability to recognize its antigen (Fig. 4). We also wanted to assessthe impact of PEGylation on Ab. It appeared that the addition of PEG-Maleimide on the Ab (Ab-PEG-Maleimide) prevented its interaction with its target.

We reasoned that if the unspecific multi-pegylation of the Ab was responsible for the loss of response of the Ab-PEG-Maleimide, then decreasing the number of thiols on the Ab could overcome its inactivation. The hypothesis was that if less PEG-Maleimide chains were grafted on the Ab, its activity might be less affected. Thus, different concentrations of IMT were used for the Ab thiolation but the interaction between the modified Ab and its target remained poor, regardless of the concentration of IMT used (supplementary data Fig. 2.S).

While these approaches are primarily used and reported in the literature for other types of nanoparticles (Altieri et al. 2019; Khayrani et al. 2019; Oh et al. 2010), our data showed that they were poorly efficient as far as Ab grafting on LNC surface was concerned. An alternative strategy was thus used to graft the Ab at LNC surface using click chemistry.

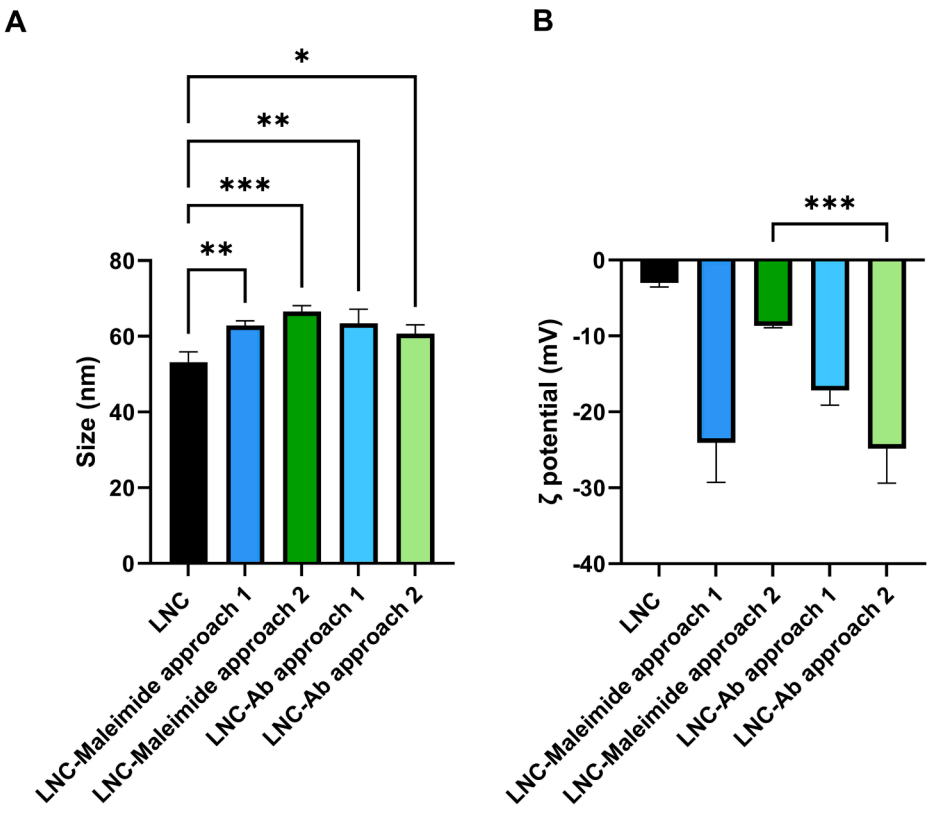


Fig. 3. Impact of transacylation and post-insertion of PEG-Maleimide on the physico-chemical properties of LNC Following transacylation ofNH_2-PEG-Maleimide (approach 1) or post-insertion of DSPE-PEG-Maleimide (approach 2) of the LNC, the Ab was linked to the LNC-Maleimides. LNC size (A) and Zeta potential (B) were measured, in water, using a Nanosizer. The values were presented as mean ± SD (N = 3, n = 3). Statistical significance was determined by a one-way ANOVA test, *p < 0.05.

Table 1
Impact of PEG-Maleimide insertion method on Ab grafting efficiency. The values are presented as mean ± SD (N = 3).

Formulations	Molar Ratio of Maleimide / Kolliphor HS®	Quantity of antibody added at the beginning of the reaction (µg)	Grafting efficiency (%)	Number of antibodies per LNC
LNC-Ab approach 1	1:100	28	66 ± 9	49 ± 1
LNC-Ab approach 2	1:100	28	38 ± 7	7 ± 4

3.4. Impact of the click chemistry method on Ab activity

A third strategy, based on click chemistry, was explored as an alternative to the maleimide-thiol coupling (approach 3) (van Geel et al. 2015).

The grafting of a PEG-DBCO polymer at LNC surface increased LNC size and decreased its zeta potential, similarly to what was observed following the addition of the maleimide conjugate with Approach 1 (Table 2). Adding the azido-modified Ab did not modify LNC size, but significantly ($p < 0,05$) increased LNC zeta potential from −28 mV to −19 mV.

When using a 1:100 M ratio of PEG-DBCO: Kolliphor HS®, no Ab was detected using primary amine quantification. As it is selective, click-chemistry offers less linkage sites. Thus, to compensate the lower amount of linking sites, the ratio of PEG-DBCO: Kolliphor HS® was increased to 1:50. Using this molar ratio, an average of 5 ± 3 Ab per LNC was obtained (23 ± 7 % of grafting efficiency).

Ab azido-modification (Ab-N_3) and PEGylation using PEG-DBCO (Ab-PEG-DBCO) did not affect Ab interaction with the PDGFRα (Fig. 5A). When the Ab was grafted on LNC surface,using approach 3, the Ab was still able to recognize its target, albeit to a lesser extent than the unmodified Ab (Fig. 5B). This grafting strategy was consequently used for the following experiments.

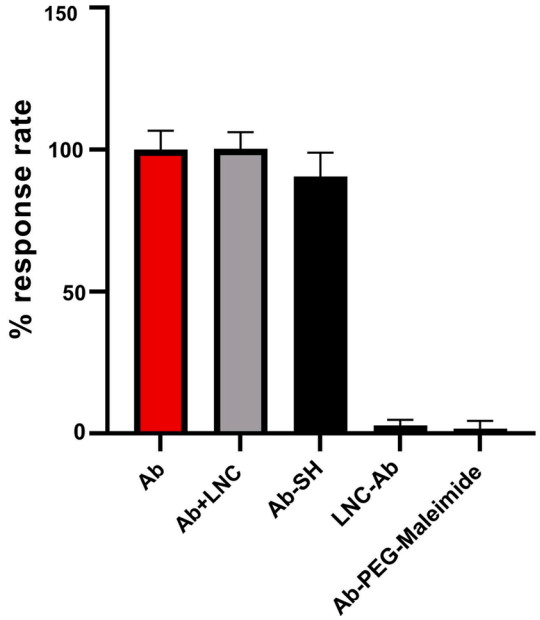


Fig. 4. Impact of Ab grafting to the surface of the LNC (approach 1) on its interaction with PDGFRα. An ELISA was used to determine the interaction between the Ab and its target protein (PDGFRα). Data are shown as a percentage of 1 nM Ab response to 20 nM of PDGFRα. All percentages were calculated relatively to unmodified anti-PDGFRα. In all conditions, Ab was at 1 nM. The values were presented as mean ± SD (N = 3, with 3 different batches of LNC-Ab, Ab-PEG-Maleimide, and Ab-SH).

Table 2
Impact of Ab grafting using Approach 3 on LNC physicochemical properties.

Formulations	Size (nm)	PDI	Zeta-Potential (mV)
LNC	58 ± 3	0.04 ± 0.03	−3 ± 0.6
LNC-DBCO	66 ± 2	0.11 ± 0.09	−28 ± 3
LNC-Ab (approach 3)	67 ± 1	0.11 ± 0.10	−19 ± 2

Size, PDI and Zeta potential were measured by Nanosizer in water. The values were presented as mean ± SD (N = 3, n = 3). Statistical significance was determined by a one-way ANOVA test, *p < 0.05.

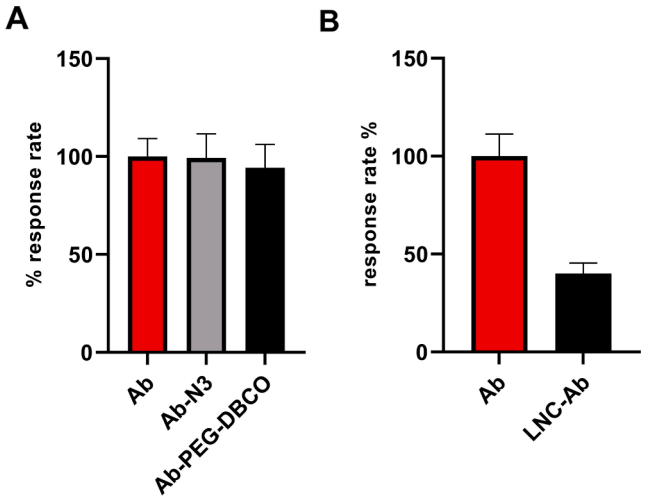


Fig. 5. Impact of Ab grafting with approach 3 on its interaction with PDGFRα. An ELISA was used to determine the interaction between the Ab and its target protein (PDGFRα) for (A) modified Ab and (B) Ab grafted on the LNC. Data are shown as a percentage of 1 nM Ab response to 20 nM of PDGFRα. All percentage were calculated relatively to Ab (unmodified anti-PDGFRα). The values were presented as mean ± SD (N = 3, with 3 different batches of LNC-Ab, Ab-N_3 and Ab-PEG-DBCO).

3.5. Impact of Ab grafting at LNC surface on LNC interactions with OPC

This part of the study aimed to characterize the interactions between LNC-Ab obtained with Approach 3 and OPC *in vitro*.

First, LNC impact on OPC viability was evaluated. The highest nontoxic concentration was 0.31 mg/ml of LNC for 1 and 4 h of incubation (Fig. 6). However, LNC were toxic (no metabolic activity) for OPC after 24 h of incubation whatever the concentration (data not shown).

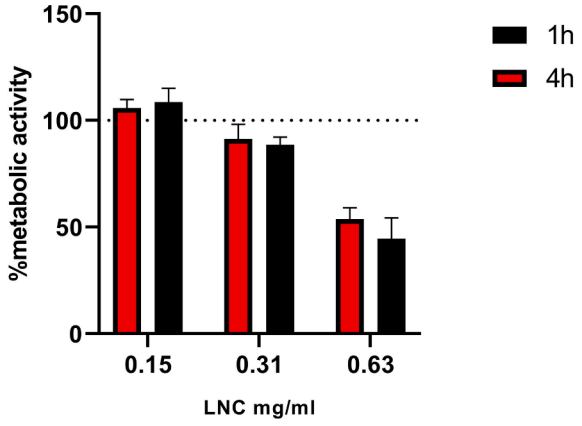


Fig. 6. Effect of LNC on OPC viability. OPC were incubated in the presence of LNC for 1 and 4 h before assessment of their viability using PrestoBlue® Cell Viability Reagent. The dotted line represents 100% of living cell and corresponds to untreated OPC. The values were presented as mean ± SD (N = 3, n = 4).

Then, DiD-loaded LNC-Ab, in conjunction with confocal microscopy and FACS, were used to assess whether LNC-Ab were able to interact with OPC. As illustrated by Fig. 7, LNC (DiD)-Ab were mainly visible in the cytoplasm of OPC, supporting their ability to enter these cells. Additional pictures of OPC treated with LNC (DiD)-Ab and negative control (untreated OPC) can be found in supplementary data (Fig. 3.S).

FACS was then used to quantify the amount of LNC associated with OPC and whether the Ab at LNC surface would increase LNC/OPC association compared to unmodified LNC. As shown in Fig. 8, grafting of the PDGFRα Ab at LNC surface allowed to increase by 1.5-fold their association with OPC.

As modifying the surface of a nanomedicine can strongly influence its interaction with cells (Yu et al. 2012; Lorenz et al. 2006), this part aimed to determine whether the increased interaction of LNC-Ab with OPC was specific of the anti-PDGFRα or was linked to LNC surface modification due to an antibody grafting. Thus, OPC association with LNC-Ab was compared with LNC grafted with an isotype control (LNC-IgG2a). It appeared that grafting the isotype control had the same effect than grafting the anti-PDGFRα (Fig. 8). Finally, to determine if LNC-Ab interactions with OPC could be affected by the presence of PDGFAA in the culture medium (PDGFRα endogenous ligand), the same experiment was repeated but without PDGFAA (i.e. the ligand of the receptor targeted by the Ab). However, the results were the same as the ones obtained in the presence of PDGFAA (Fig. 9).

4. Discussion

Nowadays, the only treatments available for multiple sclerosis are immunomodulatory therapies with mostly a peripheral action. Although they limit the burden of the symptoms, none of them stimulate the remyelination process (McGinley, Goldschmidt, and Rae-Grant 2021). This is why, for the last decades, researchers have developed strategies to promote remyelination, notably by inducing OPC differentiation into myelinating oligodendrocytes. Nevertheless, these therapies need to be efficiently delivered to OPC to be effective, and this aspect remains challenging. Hence, our goal was to improve the efficiency of pro-remyelinating therapies by improving their delivery and selectivity towards OPC. To do so, we selected lipid-based nanocarriers and we grafted an anti-PDGFRα at their surface to specifically target OPC. In the present work, for the first time, we successfully grafted an anti-PDGFRα at LNC surface, comparing two strategies: thiol-maleimide interaction and copper less click-chemistry. We were also able to quantify Ab at LNC surface, and for the first time, to demonstrate that modification of LNC surface by an antibody affected their uptake by OPC.

The thiol-maleimide chemistry is a classic technique widely used to modify nanoparticle surface (Martinez-Jothar et al. 2018). To attach the maleimide moiety, we used two approaches already described in the literature, transacylation (approach 1) and post-insertion (approach 2). The transacylation of NH_2-PEG-Maleimide has never been used to graft an antibody at LNC surface. However, transacylation itself has been used to functionalize LNC surface with chitosan by Messaouidi et al. (Messaoudi et al. 2014). We observed an increase of LNC size and a decrease of zeta potential after post-insertion of DSPE-PEG-Maleimide. Perrier et al. reported similar observations (Perrier et al. 2010) after the post-insertion of DPSE-PEG-OCH_3. However, in the work of Béduneau et al., after post-insertion of DPSE-PEG-Maleimide, the size of LNC increased to a lesser extent in our case (+24 nm vs. + 7 nm in our study) (Béduneau et al. 2007). This might be explained by the smaller amount of maleimide moiety used in our work (50-fold lower).

To compare the different approaches regarding grafting efficiency, a reliable method to quantify the Ab at LNC surface was essential. Unfortunately, LNC interacted with most of the classical used methods for proteic ligand quantification or detection at a nanoparticle surface (i.e., Bradford, RMN, SDS PAGE…) (Jahan and Haddadi 2015; Kirpotin et al. 2012; Perera et al. 2020), inducing a strong background signal (data not

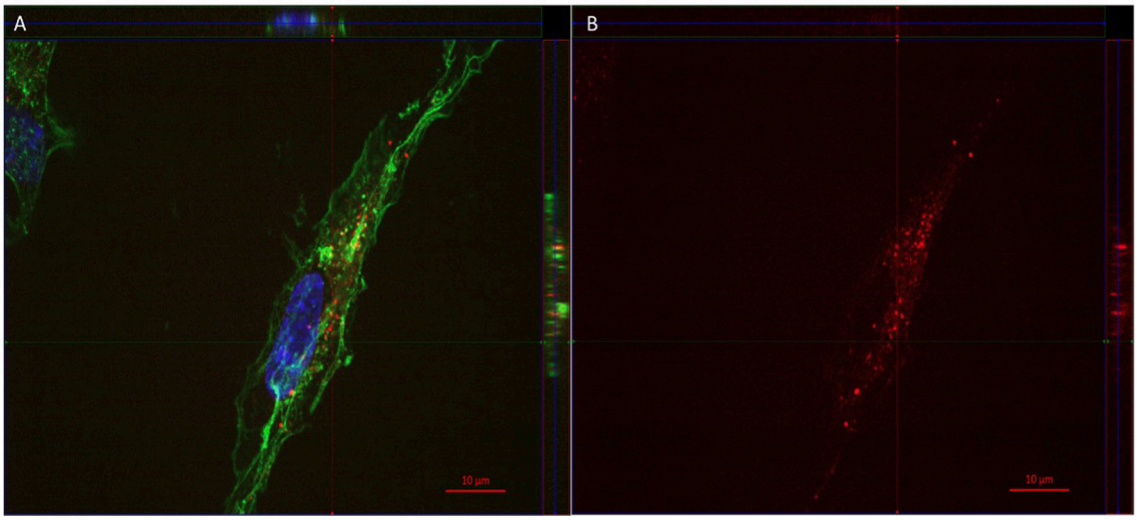


Fig. 7. Visualization of LNC-Ab localization in OPC. Representative picture of LNC localization in OPC. LNC-Ab were diluted to 0.42 mg/ml in OPC media and incubated 1 h with the cells. Blue is DAPI for cell nucleus; green is Alexa 488-Phalloidine, for F-actin, cytoskeleton; red is DiD for LNC.(A) Merged image of y − z, x − z, and z − y sections; (B) DiD-labeled LNC image of y − z, x − z, and z − y sections.

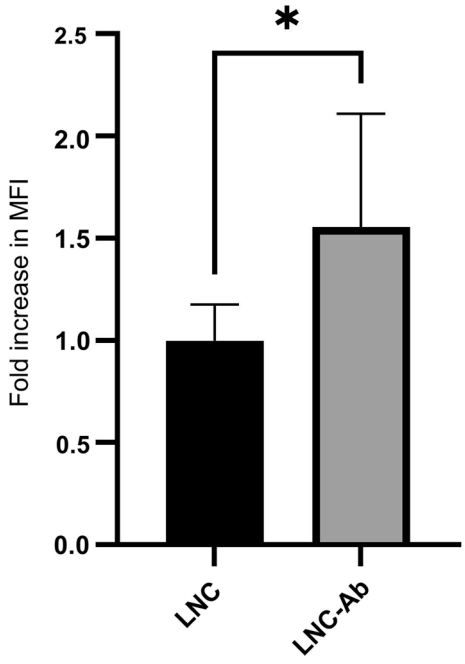


Fig. 8. Impact of anti-PDGFRα grafting on LNC OPC-associated fluorescence. DiD-Loaded LNC were incubated for 30 min with OPC at a concentration of 0.15 mg/ml. The fold increase in Mean Fluorescence Intensity per cell (MFI) was calculated relatively to LNC's MFI. Statistical significance was calculated based on an unpaired *t*-test *p < 0.05. The values were presented as mean ± SD (N = 3, n = 3).

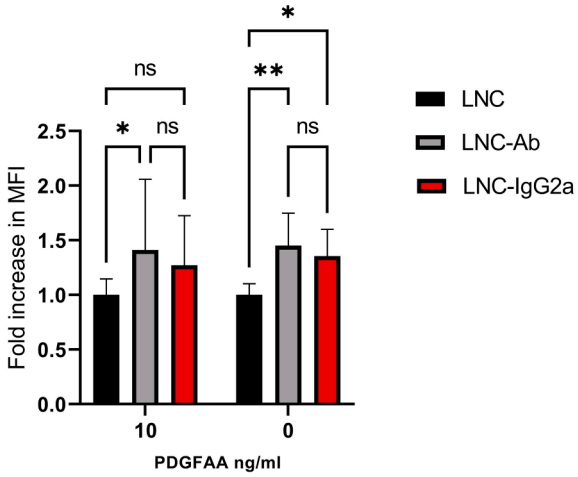


Fig. 9. Impact of LNC-Ab and LNC-IgG2a uptake by OPCs in the presence of PDGFAA in the media. Statistical significance was calculated based on a two-way ANOVA*p < 0.05, **p < 0,01. The values were presented as mean ± SD (N = 3, n = 3).

shown). Only the method developed by Schelte et al., based on primary amine quantification, allowed the direct quantification of the Ab at LNC surface without interferences (Schelte et al. 2000). To our knowledge, this is the first time that this methodology has been used to quantify an antibody at LNC surface and represent a real asset for surface modification characterization of LNC with a proteic moiety. We observed that transacylation provided the highest grafting efficiency compared to post-insertion. As transacylation linked the maleimide moiety covalently to LNC surface when post-insertion only incorporated it in the LNC shell, we hypothesized that either more maleimide moieties were attached to LNC, as the whole LNC surface was accessible, or/and that the association was more stable in case of transacylation. To our knowledge, no other work has been published concerning the grafting of an antibody on LNC surface using the transacylation of NH_2-PEG-Maleimide, and no other study directly compared post-insertion and transacylation. Béduneau et al. successfully grafted an antibody at the surface of LNC using post-insertion and calculated that +/- 67 antibodies were incorporated in LNC, but they used an indirect quantification (Béduneau et al. 2007).

Chemical modification of antibodies occurring during grafting can hinder their ability to associate with their antigen. We found that thiolation of antibody's lysines with IMT did not decrease Ab response level. However, the subsequent PEGylation of the thiol residues resulted in the loss of Ab activity. Our results suggest that PEGylation very likely occurred at the Fv region of Ab upon thiolation by IMT of the lysines of the Fv region. Hence, the pegylation of the Ab most likely hindered its interaction with PDGFRα resulting in a loss of Ab activity. This could explain why LNC-Ab obtained using approaches 1 were not able to interact with PDGFRα. Of note, Béduneau et al. also demonstrated that a thiolated OX26 antibody could still interact with its target, but no

investigation was made after grafting of the antibody on the nanoparticle (Béduneau et al. 2007). Kitamura et al. reported that the unspecific coupling of PEG via active ester on an antibody led to a decrease of 90% of the antibody activity (Kitamura et al. 1990). The decrease was linked to the number of PEG on the antibody and their molecular weight, reinforcing the hypothesis of a steric hindrance (Kitamura et al. 1990; Chapman 2002). This is why we finally used a more specific approach involving click-chemistry. While fewer Ab were grafted per LNC, nor its azido modification nor its PEGylation affected the Ab association with PDGFRα. Gai et al. modified an anti-CD11 Ab using the same strategy and observed no impact of the azido modification on the anti-CD11 functional integrity compared to the native antibody (Gai et al. 2020). Taken together, our data and those reported by others put forth a site-specific modification strategy for Ab grafting.

Nonetheless, we found that once on LNC surface the Ab response level decreased of 40%. We hypothesized that this could be due to a steric hindrance created by the LNC, mainly via the PEG moieties at its surface, as they could prevent the Ab from reaching its target. Interestingly, Botosa et al. observed a similar phenomenon with PEGylated liposomes. They demonstrated, using surface plasmon resonance, that antibody-functionalized liposomes could interact with their antigen, whereas PEGylated antibody functionalized liposomes had a decreased interaction with the antigen. They showed that it was related to PEGylated lipid fraction and PEG molecular weight (Botosoa et al. 2011).

The association of LNC-Ab with primary OPC cultures was higher than LNC but the extent of this increase was more modest than we hoped for. As OPC uptook LNC quite quickly (87% of the cells were DiD positive after 30 min of incubation only) the advantage conferred by the Ab was more difficult to highlight. While the uptake of the lipid-based nanoparticles by OPC is not extensively studied, Osorio-Querejeta et al. found that primary OPC endocytosed liposomes to a greater extent than PLGA nanoparticles and exosomes (96%, 83 %, and 61%, respectively) (Osorio-Querejeta et al. 2020). This tropism for lipid-based nanoparticles is likely due to the involvement of several unspecific endocytosis pathways, as reported for other types of cells. For instance, it has been shown that vectorized LNC with the NFL-TBS.40–63 peptide use clathrin-, caveolin-, and micropinocytosis-mediated pathways to enter oligodendrocytes (Fressinaud et al. 2020), whereas for monocytes they use mostly caveolae-mediated endocytosis and pinocytosis (Pinton et al. 2020).

For the targeting to be efficient, LNC need to enter OPC primarily by specific receptor-mediated endocytosis rather than by unspecific pathways such as those mentioned above. The antibody addition only induced a slight increase in uptake. Probably because the uptake occurring through receptor-mediated endocytosis is negligible compared to the other pathways. It can be speculated that a nanoparticle with a lower tropism for OPC would have been more suitable to target OPC, as receptor-mediated endocytosis would have been the most significant route to penetrate the cell. As many studies have demonstrated that different types of nanoparticles have different uptake rates for the same cell line (Behzadi et al. 2017), this strategy could be considered for future experiments.

Lastly, we observed that grafting an isotype control produced the same increase in LNC - OPC association as grafting the anti-PDGFRα antibody. While this critical control is lacking in many papers, Walters et al. showed that the grafting of an isotype control on PLGA nanoparticle surface increased their cell association compared to the unmodified nanoparticle (Walters et al. 2015). We can hypothesize that this could be due to the interaction of the Fc region with the immunoglobulin Fc receptors (FcR). These receptors are traditionally at the surface of immune cells, such as macrophages and monocytes, but are also present at OPC surface (especially the γ subunit) (Nakahara et al. 2003). Hence, having an antibody at LNC surface may have unlocked receptor-mediated endocytosis via the FcR. The question remains on whether increasing the anti-PDGFRα at LNC surface is required to reach a threshold allowing to differentiate between Ab and control isotype as suggested by some studies (Bruckner et al. 2021).

5. Conclusion

In summary, we produced anti-PDGFRα functionalized LNC to target OPC to favor remyelination and reduce off-target effects by targeting OPC. To graft the antibody, we used three different approaches (transacylation, post-insertion of maleimide moiety and finally coperless click-chemistry). To evaluate the anti-PDGFRα grafting efficiency on LNC, we used primary amine quantification. This method can be considered as a real asset to quantify the amount of functionalized protein moiety on LNC since these nanoparticles interfere with classical protein quantification techniques. We also developed an in-house ELISA to gauge the anti-PDGFRα activity after grafting on LNC. Our results demonstrated that site-selective antibody grafting on nanoparticles was the best way to maintain its activity. Nevertheless, *in vitro* uptake by primary OPC was only modestly increased by the Ab grafting and to the same extent as isotype control-grafted LNC. This observation highlights how crucial appropriate control is for uptake studies involving nanoparticle surface modification and how this modification impacts cell-nanoparticle interaction.

CRediT authorship contribution statement

Yasmine Labrak: Conceptualization, Data curation, Formal analysis, Writing – original draft, Methodology, Investigation. **Béatrice Heurtault:** Resources, Validation, Investigation. **Benoît Frisch:** Methodology. **Patrick Saulnier:** Methodology. **Elise Lepeltier:** Methodology. **Veronique E Miron:** Methodology. **Giulio G. Muccioli:** Methodology, Conceptualization, Project administration, Supervision, Writing – review & editing. **Anne des Rieux:** Conceptualization, Funding acquisition, Project administration, Supervision, Writing – review & editing.

Declaration of Competing Interest

The authors declare that they have no known competing financial interests or personal relationships that could have appeared to influence the work reported in this paper.

Acknowledgments

Yasmine Labrak is a F.R.S.-FNRS (Fonds de la recherche scientifique) FRIA grant holder. Anne des Rieux is a F.R.S.-FNRS Senior Research Associate. Anne des Rieux was recipient of a grant from the foundation Charcot. The authors would like to thank Dr. Nicolas Dauguet for his help regarding FACS data analysis and Dr. Leopold Thabault for scientific discussions. In memory of a beloved friend, Françoise Lemoine, who died from MS. Illustrations were created using Biorender.com

Appendix A. Supplementary material

Supplementary data to this article can be found online at https://doi.org/10.1016/j.ijpharm.2022.121623.

References

Altieri, F., Cairone, F., Giamogante, F., Carradori, S., Locatelli, M., Chichiarelli, S., Cesa, S., 2019. Influence of Ellagitannins Extracted by Pomegranate Fruit on Disulfide Isomerase PDIA3 Activity. Nutrients 11.

Bastiat, G., Pritz, C.O., Roider, C., Fouchet, F., Lignières, E., Jesacher, A., Glueckert, R., Ritsch-Marte, M., Schrott-Fischer, A., Saulnier, P., Benoit, J.-P., 2013. A new tool to ensure the fluorescent dye labeling stability of nanocarriers: a real challenge for fluorescence imaging. J. Control Release 170 (3), 334–342.

Béduneau, A., Saulnier, P., Hindré, F., Clavreul, A., Leroux, J.-C., Benoit, J.-P., 2007. Design of targeted lipid nanocapsules by conjugation of whole antibodies and antibody Fab' fragments. Biomaterials 28, 4978–4990.

Behzadi, S., Serpooshan, V., Tao, W., Hamaly, M.A., Alkawareek, M.Y., Dreaden, E.C., Brown, D., Alkilany, A.M., Farokhzad, O.C., Mahmoudi, M., 2017. Cellular uptake of nanoparticles: journey inside the cell. Chem. Soc. Rev. 46, 4218–4244.

Botosoa, E.P., Maillasson, M., Mougin-Degraef, M., Remaud-Le Saëc, P., Gestin, J.-F., Jacques, Y., Barbet, J., Faivre-Chauvet, A., 2011. Antibody-Hapten Recognition at the Surface of Functionalized Liposomes Studied by SPR: Steric Hindrance of Pegylated Phospholipids in Stealth Liposomes Prepared for Targeted Radionuclide Delivery. J. Drug Deliv. 2011, 1–9.

Brown, J.W.L., Cunniffe, N.G., Prados, F., Kanber, B., Jones, J.L., Needham, E., Georgieva, Z., Rog, D., Pearson, O.R., Overell, J., MacManus, D., Samson, R.S., Stutters, J., ffrench-Constant, C., Gandini Wheeler-Kingshott, C.A.M., Moran, C., Flynn, P.D., Michell, A.W., Franklin, R.J.M., Chandran, S., Altmann, D.R., Chard, D. T., Connick, P., Coles, A.J., 2021. Safety and efficacy of bexarotene in patients with relapsing-remitting multiple sclerosis (CCMR One): a randomised, double-blind, placebo-controlled, parallel-group, phase 2a study. Lancet Neurol 20 (9), 709–720.

Bruckner, M., Simon, J., Landfester, K., Mailander, V., 2021. The conjugation strategy affects antibody orientation and targeting properties of nanocarriers. Nanoscale 13, 9816–9824.

Carradori, D., P. Saulnier, V. Preat, A. des Rieux, and J. Eyer. 2016. 'NFL-lipid nanocapsules for brain neural stem cell targeting in vitro and in vivo', *J Control Release*, 238: 253-62.

Chapman, A.P., 2002. PEGylated antibodies and antibody fragments for improved therapy: a review. Adv. Drug Deliv. Rev. 54, 531–545.

Dendrou, C.A., Fugger, L., Friese, M.A., 2015. Immunopathology of multiple sclerosis. Nat. Rev. Immunol. 15 (9), 545–558.

Dobson, R., and G. Giovannoni. 2019. "Multiple sclerosis – a review." In.

Filippi, M., Bar-Or, A., Piehl, F., Preziosa, P., Solari, A., Vukusic, S., Rocca, M.A., 2018. Multiple sclerosis. Nat. Rev. Dis. Primers 4, 43.

Franklin, Robin J. M., and Charles Ffrench-Constant. 2017. "Regenerating CNS myelin - From mechanisms to experimental medicines." In.

Fressinaud, C., Thomas, O., Umerska, A.M., Saulnier, P., 2020. Lipid Nanoparticles Vectorized with NFL-TBS.40-63 Peptide Target Oligodendrocytes and Promote Neurotrophin-3 Effects After Demyelination In Vitro. Neurochem Res 45 (11), 2732–2748.

Gai, M., Simon, J., Lieberwirth, I., Mailänder, V., Morsbach, S., Landfester, K., 2020. A bio-orthogonal functionalization strategy for site-specific coupling of antibodies on vesicle surfaces after self-assembly. Polym. Chem. 11 (2), 527–540.

Gazaille, C., Sicot, M., Akiki, M., Lautram, N., Dupont, A., Saulnier, P., Eyer, J., Bastiat, G., 2021. Characterization of Biological Material Adsorption to the Surface of Nanoparticles without a Prior Separation Step: a Case Study of Glioblastoma-Targeting Peptide and Lipid Nanocapsules. Pharm. Res. 38 (4), 681–691.

Göttle, P., Förster, M., Weyers, V., Küry, P., Rejdak, K., Hartung, H.-P., Kremer, D., 2019. An unmet clinical need: roads to remyelination in MS. Neurol. Res. Pract. 1 (1) https://doi.org/10.1186/s42466-019-0026-0.

Heurtault, Béatrice, Patrick Saulnier, Brigitte Pech, Jacques Emile Proust, and Jean Pierre Benoit. 2002. 'A novel phase inversion-based process for the preparation of lipid nanocarriers', *Pharmaceutical Research*.

Hirsjarvi, S., Belloche, C., Hindre, F., Garcion, E., Benoit, J.P., 2014. Tumour targeting of lipid nanocapsules grafted with cRGD peptides. Eur. J. Pharm. Biopharm. 87, 152–159.

Jahan, S.T., Haddadi, A., 2015. Investigation and optimization of formulation parameters on preparation of targeted anti-CD205 tailored PLGA nanoparticles. Int J Nanomedicine 10, 7371–7384.

Khayrani, A.C., Mahmud, H., Oo, A.K.K., Zahra, M.H., Oze, M., Du, J., Alam, M.J., Afify, S.M., Quora, H.A.A., Shigehiro, T., Calle, A.S., Okada, N., Seno, A., Fujita, K., Hamada, H., Seno, Y., Mandai, T., Seno, M., 2019. Targeting Ovarian Cancer Cells Overexpressing CD44 with Immunoliposomes Encapsulating Glycosylated Paclitaxel. Int. J. Mol. Sci. 20.

Kirpotin, D.B., Noble, C.O., Hayes, M.E., Huang, Z., Kornaga, T., Zhou, Y., Nielsen, U.B., Marks, J.D., Drummond, D.C., 2012. Building and characterizing antibody-targeted lipidic nanotherapeutics. Methods Enzymol. 502, 139–166.

Kitamura, K., Takahashi, T., Takashina, K., Yamaguchi, T., Noguchi, A., Tsurumi, H., Toyokuni, T., Hakomori, S., 1990. Polyethylene glycol modification of the monoclonal antibody A7 enhances its tumor localization. Biochem. Biophys. Res. Commun. 171, 1387–1394.

Laine, A.L., Huynh, N.T., Clavreul, A., Balzeau, J., Bejaud, J., Vessieres, A., Benoit, J.P., Eyer, J., Passirani, C., 2012. Brain tumour targeting strategies via coated ferrociphenol lipid nanocapsules. Eur. J. Pharm. Biopharm. 81, 690–693.

Li, P., Li, H.X., Jiang, H.Y., Zhu, L., Wu, H.Y., Li, J.T., Lai, J.H., 2017. Expression of NG2 and platelet-derived growth factor receptor alpha in the developing neonatal rat brain. Neural Regen. Res. 12, 1843–1852.

Lorenz, M.R., Holzapfel, V., Musyanovych, A., Nothelfer, K., Walther, P., Frank, H., Landfester, K., Schrezenmeier, H., Mailander, V., 2006. Uptake of functionalized, fluorescent-labeled polymeric particles in different cell lines and stem cells. Biomaterials 27, 2820–2828.

Lubetzki, C., Zalc, B., Williams, A., Stadelmann, C., Stankoff, B., 2020. Remyelination in multiple sclerosis: from basic science to clinical translation. Lancet Neurol. 19, 678–688.

Martínez-Jothar, L., Doulkeridou, S., Schiffelers, R.M., Sastre Torano, J., Oliveira, S., van Nostrum, C.F., Hennink, W.E., 2018. Insights into maleimide-thiol conjugation chemistry: Conditions for efficient surface functionalization of nanoparticles for receptor targeting. J. Control Release 282, 101–109.

McGinley, M.P., Goldschmidt, C.H., Rae-Grant, A.D., 2021. Diagnosis and Treatment of Multiple Sclerosis: A Review. JAMA 325 (8), 765. https://doi.org/10.1001/jama.2020.26858.

Messaoudi, K., Saulnier, P., Boesen, K., Benoit, J.P., Lagarce, F., 2014. Anti-epidermal growth factor receptor siRNA carried by chitosan-transacylated lipid nanocapsules increases sensitivity of glioblastoma cells to temozolomide. Int. J. Nanomed.

Miron, V.E., Boyd, A., Zhao, J.-W., Yuen, T.J., Ruckh, J.M., Shadrach, J.L., van Wijngaarden, P., Wagers, A.J., Williams, A., Franklin, R.J.M., ffrench-Constant, C., 2013. M2 microglia and macrophages drive oligodendrocyte differentiation during CNS remyelination. Nat. Neurosci. 16 (9), 1211–1218.

Morille, M., Passirani, C., Letrou-Bonneval, E., Benoit, J.P., Pitard, B., 2009. Galactosylated DNA lipid nanocapsules for efficient hepatocyte targeting. Int. J. Pharm. 379, 293–300.

Nakahara, J., Tan-Takeuchi, K., Seiwa, C., Gotoh, M., Kaifu, T., Ujike, A., Inui, M., Yagi, T., Ogawa, M., Aiso, S., Takai, T., Asou, H., 2003. Signaling via immunoglobulin Fc receptors induces oligodendrocyte precursor cell differentiation. Dev Cell 4, 841–852.

Oh, E., Susumu, K., Blanco-Canosa, J.B., Medintz, I.L., Dawson, P.E., Mattoussi, H., 2010. Preparation of stable maleimide-functionalized au nanoparticles and their use in counting surface ligands. Small 6, 1273–1278.

Osorio-Querejeta, I., S. Carregal-Romero, A. Ayerdi-Izquierdo, I. Mager, N. L. A, M. Wood, A. Egimendia, M. Betanzos, A. Alberro, L. Iparraguirre, L. Moles, I. Llarena, M. Moller, F. Goni-de-Cerio, G. Bijelic, P. Ramos-Cabrer, M. Munoz-Culla, and D. Otaegui. 2020. 'MiR-219a-5p Enriched Extracellular Vesicles Induce OPC Differentiation and EAE Improvement More Efficiently Than Liposomes and Polymeric Nanoparticles', *Pharmaceutics*, 12.

Perera, Y.R., South, T.M., Hughes, A.C., Parkhurst, A.N., Williams, O.C., Davidson, M.B., Wilks, C.A., Mlsna, D.A., Fitzkee, N.C., 2020. Using NMR Spectroscopy To Measure Protein Binding Capacity on Gold Nanoparticles. J. Chem. Educ. 97, 820–824.

Perrier, T., Saulnier, P., Fouchet, F., Lautram, N., Benoît, J.-P., 2010. Post-insertion into Lipid NanoCapsules (LNCs): From experimental aspects to mechanisms. Int. J. Pharm. 396 (1-2), 204–209.

Pinton, L., Magri, S., Masetto, E., Vettore, M., Schibuola, I., Ingangi, V., Marigo, I., Matha, K., Benoit, J.P., Della Puppa, A., Bronte, V., Lollo, G., Mandruzzato, S., 2020. Targeting of immunosuppressive myeloid cells from glioblastoma patients by modulation of size and surface charge of lipid nanocapsules. J. Nanobiotechnol. 18, 31.

Roger, E., Gimel, J.C., Bensley, C., Klymchenko, A.S., Benoit, J.P., 2017. Lipid nanocapsules maintain full integrity after crossing a human intestinal epithelium model. J. Control Release 253, 11–18.

Schelté,, P., Boeckler, C., Frisch, B., Schuber, F., 2000. Differential reactivity of maleimide and bromoacetyl functions with thiols: application to the preparation of liposomal diepitope constructs. Bioconjug. Chem. 11 (1), 118–123.

Udenfriend, S., Stein, S., Böhlen, P., Dairman, W., Leimgruber, W., Weigele, M., 1972. Fluorescamine: A reagent for assay of amino acids, peptides, proteins, and primary amines in the picomole range. Science 178 (4063), 871–872.

Umerska, A., Matougui, N., Groo, A.C., Saulnier, P., 2016. Understanding the adsorption of salmon calcitonin, antimicrobial peptide AP114 and polymyxin B onto lipid nanocapsules. Int. J. Pharm. 506, 191–200.

van Geel, R., Wijdeven, M.A., Heesbeen, R., Verkade, J.M., Wasiel, A.A., van Berkel, S.S., van Delft, F.L., 2015. Chemoenzymatic Conjugation of Toxic Payloads to the Globally Conserved N-Glycan of Native mAbs Provides Homogeneous and Highly Efficacious Antibody-Drug Conjugates. Bioconjug. Chem. 26, 2233–2242.

Walters, A.A., Somavarapu, S., Riitho, V., Stewart, G.R., Charleston, B., Steinbach, F., Graham, S.P., 2015. Assessment of the enhancement of PLGA nanoparticle uptake by dendritic cells through the addition of natural receptor ligands and monoclonal antibody. Vaccine 33 (48), 6588–6595.

Xu, Y., Carradori, D., Alhouayek, M., Muccioli, G.G., Cani, P.D., Preat, V., Beloqui, A., 2018. Size Effect on Lipid Nanocapsule-Mediated GLP-1 Secretion from Enteroendocrine L Cells. Mol. Pharm. 15, 108–115.

Yu, S.S., Lau, C.M., Thomas, S.N., Jerome, W.G., Maron, D.J., Dickerson, J.H., Hubbell, J. A., Giorgio, T.D., 2012. Size- and charge-dependent non-specific uptake of PEGylated nanoparticles by macrophages. Int. J. Nanomed. 7, 799–813.

Zou, J., Saulnier, P., Perrier, T., Zhang, Y.a., Manninen, T., Toppila, E., Pyykkö, I., 2008. Distribution of lipid nanocapsules in different cochlear cell populations after round window membrane permeation. J. Biomed. Mater. Res. Part B Appl. 87B (1), 10–18.